

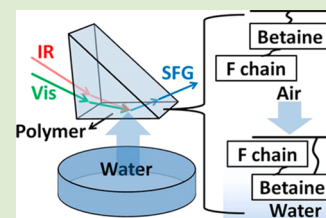
# In Situ Probing the Surface Restructuring of Antibiofouling Amphiphilic Polybetaines in Water

Chuan Leng,<sup>†</sup> Katherine A. Gibney,<sup>‡</sup> Yuwei Liu,<sup>†</sup> Gregory N. Tew,<sup>\*,‡</sup> and Zhan Chen<sup>\*,†</sup>

<sup>†</sup>Department of Chemistry, University of Michigan, Ann Arbor, Michigan 48109, United States

<sup>‡</sup>Department of Polymer Science and Engineering, Conte Research Center, University of Massachusetts, Amherst, Massachusetts 01003, United States

**ABSTRACT:** Antibiofouling materials have a wide range of applications in biomedical devices and marine coatings. Due to the amphiphilic nature of proteins and organisms, amphiphilic materials have been designed to resist their unspecific adsorption. Surface restructuring behavior of amphiphilic materials in water is believed to play a key role in the antibiofouling mechanisms. In this work, the surface structures of several amphiphilic polybetaine coatings in water have been probed in situ using sum frequency generation (SFG) vibrational spectroscopy. These are novel polybetaines constructed from functionalized polynorbornenes. The polybetaines with oligo(ethylene glycol) (OEG), octyl (C8), or fluorinated (F13) side chains exhibit different surface restructuring behaviors upon contacting water due to their different surface hydrophobicity. The OEG and C8 chains were present and ordered at the water interface, while the F13 chain withdrew from water. The hydrophilic betaine group extended into the water and formed hydrogen bonds with water molecules. The surface restructuring of these materials detected using SFG can be well correlated to their antibiofouling performance, providing an understanding of their antibiofouling mechanisms.



Antibiofouling materials have great use in a wide range of important applications from ship hulls to biomedical implants.<sup>1</sup> Poly(dimethyl siloxane) (PDMS), poly(ethylene glycol) (PEG),<sup>2</sup> and zwitterionic-based materials<sup>3</sup> have been extensively studied for fouling-release and nonsticky coatings. Solely hydrophobic or hydrophilic surfaces are believed to be inadequate to completely resist biofouling, because proteins and larger organisms are intrinsically amphiphilic and attach to surfaces with different mechanisms.<sup>4</sup> To address this issue, there is an increasing awareness that amphiphilic materials may offer superior antibiofouling properties. Such materials can resist biofouling by restructuring their surfaces depending on their environment, similar to living organisms.<sup>5</sup>

A typical amphiphilic material was reported to combine both hydrophilic PEG and hydrophobic fluorinated polymer segments, which resisted biofouling better than the sole use of PEG or fluorinated polymers.<sup>6</sup> Based on the same principle, surface active block copolymers (SABC) were synthesized with amphiphilic side chains containing both PEG and fluorinated components, which showed strong resistance to the attachment of various organisms.<sup>7–9</sup> Polypeptoids, a non-natural biomimetic polymer, have also been designed for antibiofouling. The property of the polypeptoids could be tuned by varying the amount and sequence of PEG and fluorinated blocks.<sup>10</sup> Recently, an entirely new class of amphiphilic polybetaines with different side chains were synthesized via ring-opening metathesis polymerization.<sup>11,12</sup> These materials take advantage of the hydrophilic zwitterionic functional groups while their surface properties are further tuned by hydrophilic or hydrophobic side chains (Figure 1). For example, the polybetaine containing oligo(ethylene glycol) side chain (ZI-OEG) is hydrophilic, while the polymers bearing octyl or

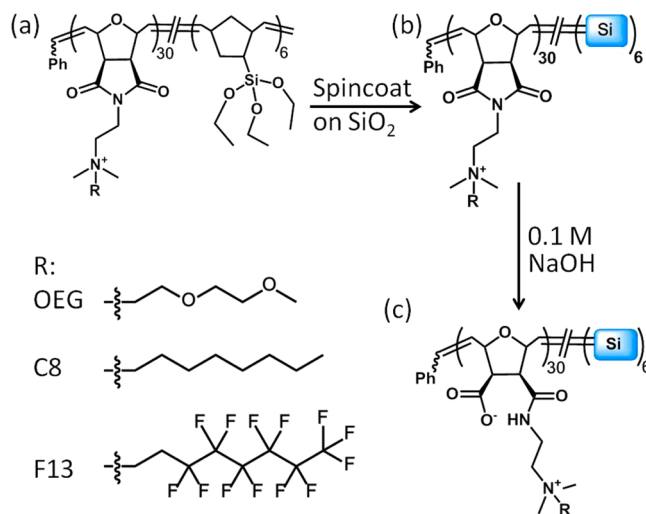


**Figure 1.** Preparation of the amphiphilic polybetaine coatings. Briefly, (a) cationic polymers were spin-coated on SiO<sub>2</sub> substrates and cured to form (b) cationic coatings, followed by hydrolysis in 0.1 M NaOH to form (c) amphiphilic coatings.

fluorinated side chains (ZI-C8 or ZI-F13) are hydrophobic. The antibiofouling assays showed that the ZI-OEG and ZI-F13 surfaces resisted the nonspecific adsorption of several types of proteins, while protein adsorption on the ZI-C8 coating was greater than the other betaines.<sup>11</sup>

**Received:** September 28, 2013

**Accepted:** October 23, 2013

**Published:** October 30, 2013

The antibiofouling capability of amphiphilic materials often depends on their surface structures in water. In previous reports, the surface structures of various polymers were determined by X-ray spectroscopy in vacuum<sup>7–9,13,14</sup> and their surface restructuring in water was deduced from atomic force microscopy and dynamic water contact angle experiments.<sup>10–12</sup> However, none of these characterization methods provided direct evidence of the polymer surface restructuring at the molecular level in water. Hence, an in situ technique is needed to probe the polymer/water interface.

Sum frequency generation (SFG) vibrational spectroscopy is an intrinsically surface sensitive and in situ vibrational spectroscopic method, providing information about chemical structures at a molecular level.<sup>15</sup> It has been extensively applied to study structures of polymers and biomolecules at various interfaces<sup>16–19</sup> and has proved to be particularly powerful in revealing polymer/water interfacial structures in ambient environments.<sup>20–23</sup> For antibiofouling coatings, SFG has been applied to probe the surfaces of biocide modified PDMS materials in water to reveal their antibiofouling mechanisms.<sup>24–26</sup>

Here, we used the same SFG spectroscopic system as reported previously.<sup>27</sup> Briefly, the visible and infrared (IR) input beams penetrate a right angle SiO<sub>2</sub> or CaF<sub>2</sub> prism and overlap spatially and temporally at the sample surface/interface, as shown in Figure 2. The incident angles of the visible and IR

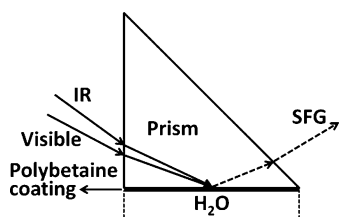


**Figure 2.** SFG sample geometry with polybetaine film on a right angle prism in contact with water.

beams are 60 and 54° with respect to the surface normal, and the pulse energies of the visible and IR beams are 30 and 100  $\mu$ J, respectively. The reflected SFG signal is collected by a monochromator along with a photomultiplier tube. All SFG spectra were collected using the ssp (SFG output, visible input, and IR input) polarization combination.

In this work, surface structures of three amphiphilic polybetaines with different side chains (Figure 1) were probed in air and water with SFG in situ. The SFG signals from the OEG, C8, and F13 side chains were obtained in air and then compared to signals from the water interface to understand their different restructuring behaviors. Moreover, the SFG signals from the betaine group showed its affinity toward water. The SFG results on the surface restructuring of the polymers in water were used to explain their antibiofouling mechanisms.

The conversion from the cationic coatings (N(+)-OEG, (N+) -C8, and N(+)-F13, Figure 1b) to the zwitterionic coatings (Figure 1c) was characterized by ATR-FTIR. The ATR-FTIR spectra collected from all cationic coating samples showed a peak at 1706  $\text{cm}^{-1}$  (Figure 3A–C) contributed from the imide group. After ring-opening in NaOH, for all coating samples, the peak at 1706  $\text{cm}^{-1}$  disappeared and two new peaks at 1587 and 1662  $\text{cm}^{-1}$  from the carboxylate or amide groups appeared (Figure 3D–F), indicating the complete conversion from the imide ring to the negatively charged carboxylate group. In addition, signals from the side chains for all the polymers were observed in the IR spectra. The peak at 1102  $\text{cm}^{-1}$  for both N(+)-OEG and ZI-OEG was assigned to the vibration of C–O–C on the OEG chain (Figure 3A,D). Both N(+)-C8 and ZI-C8 showed IR absorption at the range of 2850–2930  $\text{cm}^{-1}$  due to the alkyl chain (Figure 3B,E). For both N(+)-F13 and ZI-F13, the peaks at 1146–1238  $\text{cm}^{-1}$  were attributed to the C–F vibration (Figure 3C,F). The assignment of the peaks in the SFG spectra below.

For SFG experiments, we initially characterized the polymer surfaces in air before studying the surface restructuring in water. In the SFG spectra in the C–H stretching vibrational frequency region in air (Figure 4A), characteristic signals from the OEG and C8 side chains were observed. The peak at 2820  $\text{cm}^{-1}$  was

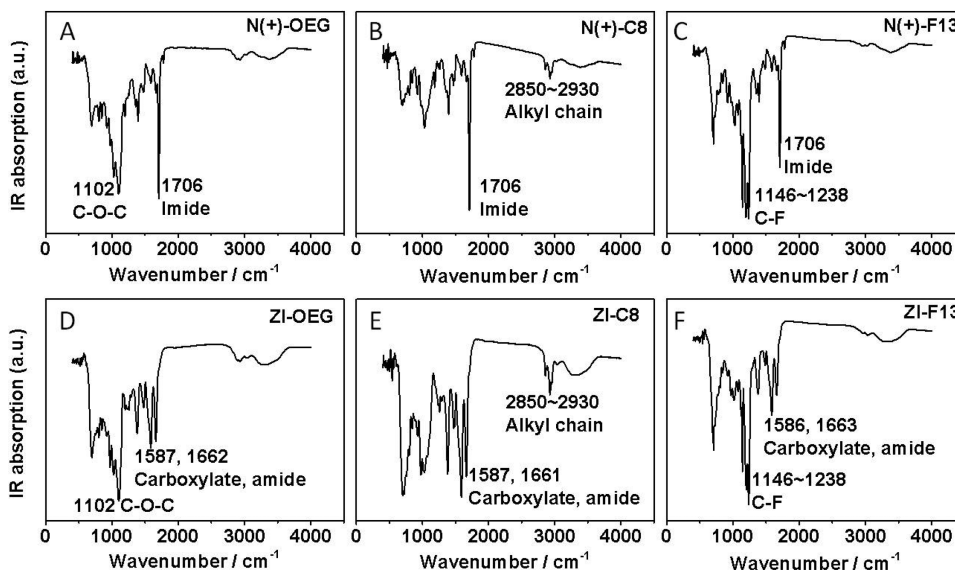


**Figure 3.** ATR-FTIR spectra of cationic (A) N(+)-OEG, (B) N(+)-C8, and (C) N(+)-F13 coatings and zwitterionic (D) ZI-OEG, (E) ZI-C8, and (F) ZI-F13 coatings.

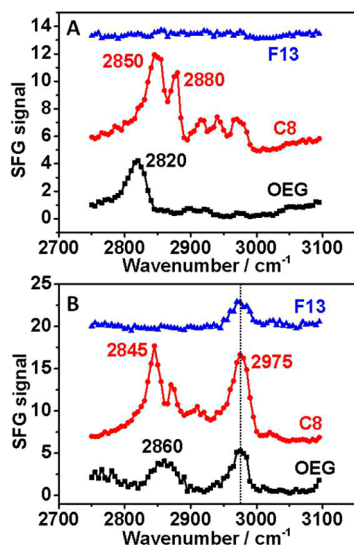


**Figure 4.** SFG spectra of ZI-OEG, ZI-C8 and ZI-F13 surfaces (A) in air and (B) in contact with D<sub>2</sub>O in the C–H stretching vibrational frequency region.

assigned to the O–CH<sub>3</sub> end group on the OEG chain.<sup>28</sup> The peaks at 2850 and 2880 cm<sup>-1</sup> were contributed from the symmetric stretching of the CH<sub>2</sub> and CH<sub>3</sub> groups on the C8 chain, respectively.<sup>29</sup> The SFG signals detected from the OEG and C8 chains indicated their presence on the coating surfaces in air. No SFG signal was observed for the ZI-F13 coating in this frequency region, showing that no ordered CH groups were present on the surface.

To study the polymer/water interfaces, D<sub>2</sub>O was used to avoid signal interference between the polymer CH groups and H<sub>2</sub>O. Figure 4B displays the SFG spectra of the interfaces between the three coatings and water. All samples exhibit a peak at 2975 cm<sup>-1</sup>, possibly from the N–CH<sub>3</sub> or N–CH<sub>2</sub> groups, indicating that the cationic quaternary amine might migrate to the surface in contact with water.

The ZI-OEG sample showed a peak at 2860 cm<sup>-1</sup>, which was contributed from the O–CH<sub>2</sub> group on the OEG chain,<sup>28</sup> indicating the presence of the OEG chain at the water interface. PEG has been extensively used to prepare antibiofouling materials due to its hydrophilicity.<sup>2,30–32</sup> Here, the OEG chain at the surface is critical to resist biofouling on the ZI-OEG coating. The ZI-C8 sample showed peaks at 2845 and 2880 cm<sup>-1</sup>, assigned to the symmetric stretching of the CH<sub>2</sub> and CH<sub>3</sub> groups, indicating that the C8 chain was present on the surface in water. The hydrophobic C8 chain was present at the water interface most likely because the C8 chain was directly connected to the quaternary amine, which has a strong affinity toward water. The C8 chain at the water interface could lead to protein adsorption by hydrophobic interactions, which explains the reported fouling properties of the ZI-C8 material.<sup>12</sup> It is worth mentioning that the 2975 cm<sup>-1</sup> signal detected from ZI-OEG and ZI-C8 may also contain some contribution from the asymmetric C–H stretching of the OCH<sub>3</sub> and CH<sub>3</sub> groups, respectively.

In addition, SFG spectra were taken for the ZI-F13 coating between 1000 and 1350 cm<sup>-1</sup> to study the C–F vibrational signals (Figure 5A). In air, a peak at 1235 cm<sup>-1</sup> was detected. According to the IR spectra (Figure 3C,F), this peak was assigned to C–F stretching from the F13 chain, again confirming the surface presence of the F13 chain in air.

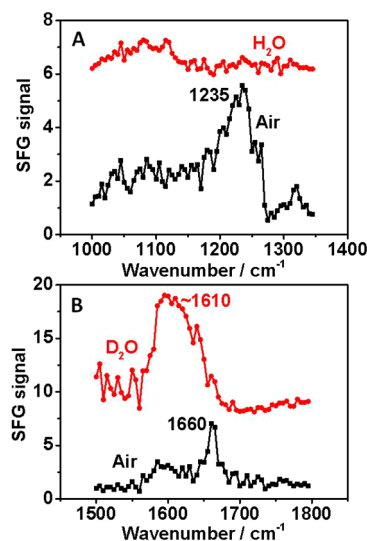


**Figure 5.** SFG spectra of the ZI-F13 coating in air and water in the (A) C–F and (B) C=O vibrational frequency region.

When the film was in contact with water, this peak disappeared, indicating that the fluorinated chain either became random or withdrew from the water interface due to the unfavorable interactions between the hydrophobic fluorinated chain and water. This result is well correlated to the SFG C–H studies of the ZI-F13 sample, where no CH groups were observed on the surface in air, however, CH signals were detected on the surface in water.

To study the surface behavior of the carboxylate group in the ZI-F13 sample, SFG spectra were collected from 1500 to 1800 cm<sup>-1</sup> in the C=O stretching vibration frequency range (Figure 5B). In air, a peak at 1660 cm<sup>-1</sup> was detected, while in water, a stronger peak around 1610 cm<sup>-1</sup> was observed. The signals here were contributed from the carboxylate group. The higher signal intensity in water than in air indicated that the carboxylate group was present and had better ordering at the water interface. The red shift of the peak from air to water could be caused by hydration or hydrogen bonding of the carboxylate group with water. The signal at 1610 cm<sup>-1</sup> could not be contributed by the amide, because the hydrogen bonding between amide and water would not shift the signal of amide to as low as 1610 cm<sup>-1</sup>.<sup>33</sup> Therefore, combining the SFG results of the ZI-F13 sample in water (Figures 4B and 5), we believe that the betaine group containing the quaternary amine and the carboxylate groups moved to the water interface while the F13 chain withdrew from water. Previously, zwitterionic polymers have been reported as promising antibiofouling materials due to their surface hydration.<sup>3,34–36</sup> Here, the exposure of the betaine group to the water interface and its hydration were responsible for resisting biofouling, as detected previously.<sup>11,12</sup>

SFG studies indicated that the three polymers with the same backbone but different side chains exhibit different surface structures in water. Surface restructurings of polymers were observed using SFG in situ. The schematics of the three polymer surfaces in water are depicted in Figure 6. The SFG results on surface restructurings are consistent with the dynamic water contact angle data that we reported previously.<sup>11</sup> The contact angle hysteresis of the ZI-F13 surface is much larger than that of the ZI-OEG and ZI-C8 surfaces, indicating its more distinct surface restructuring upon contacting water.

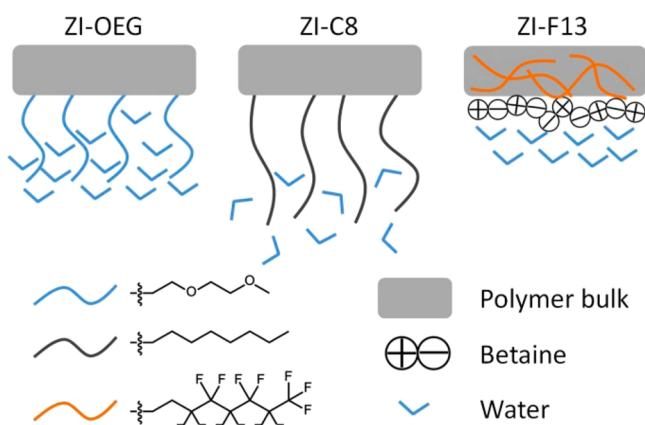


**Figure 6.** Schematic representation of the polymer surface structures in water.

To summarize, we probed the surface restructuring behavior of three polybetaines with different side chains in water using SFG spectroscopy. The SFG results showed that the side chains of the three polymers were all present on the surface in air. In water, the OEG and C8 chains remained on the coating surface, while the F13 chain withdrew from water. For ZI-F13, both the quaternary amine group and the carboxylate group were present at the water interface, where the carboxylate group formed hydrogen bonds with water molecules. The surface restructuring information obtained from the SFG data provides direct experimental evidence of the antibiofouling mechanisms of the amphiphilic materials: The good antifouling properties of ZI-OEG were due to the surface presence of the OEG groups on the surface; it has been extensively shown that the surface OEG groups lead to improved antibiofouling activity. The poor antifouling performance of the ZI-C8 was due to the surface presence of the C8 side chain, which resulted in protein adsorption due to hydrophobic interactions. The ZI-F13 also exhibited good antifouling performance, because the F13 side chain retreated to the bulk in water so that the zwitterionic groups were exposed at the surface. It has been demonstrated that zwitterionic materials can be good antibiofouling materials. This research indicates that side chains can greatly influence the polymer surface structures in water, resulting in different surface properties and thus different antibiofouling properties.

## EXPERIMENTAL SECTION

Cationic polymers with OEG, C8, and F13 side chains (N(+)-OEG, N(+)-C8, and N(+)-F13; Figure 1a) were synthesized according to our previously published method with molecular weight and compositions presented in the literature.<sup>11,12</sup> Millipore water (18.2 M $\Omega$ -cm) was used in all the experiments.

Right angle SiO<sub>2</sub> and CaF<sub>2</sub> prisms were purchased from Altos Photonics (Bozeman, MT). A layer of 100 nm SiO<sub>2</sub> was deposited onto each CaF<sub>2</sub> prism by an electron-beam deposition process using an SJ-26 Evaporator system at a pressure below 10<sup>-5</sup> Torr. The deposition rate was 5 Å/s. The SiO<sub>2</sub> prisms and SiO<sub>2</sub> coated CaF<sub>2</sub> prisms were treated with O<sub>2</sub> plasma for 4 min in a PE-25-JW plasma cleaner (Plasma Etch, Carson City, NV). The amphiphilic polybetaine coatings were prepared according to our prior report (Figure 1).<sup>11</sup> The ZI-OEG and ZI-C8 coatings were prepared on SiO<sub>2</sub> prisms, and the ZI-F13 coating was prepared on the SiO<sub>2</sub>-coated CaF<sub>2</sub> prism. The thicknesses of the spin-coated films are around 30 nm, measured by a LSE model Gaertner Scientific Stokes Ellipsometer.<sup>11,12</sup>

Attenuated total reflection Fourier transform infrared (ATR-FTIR) spectra were collected on a Thermo Scientific Nicolet 6700 spectrometer with a Harrick germanium attenuated total reflection

accessory and a liquid N<sub>2</sub>-cooled HgCdTe amplified detector. Polymer films were prepared on freshly cleaned Si surfaces, which were pressured against the germanium crystal for ATR-FTIR measurements.

## AUTHOR INFORMATION

### Corresponding Authors

\*E-mail tew@mail.pse.umass.edu. Fax 413-545-2873.

\*E-mail zhanc@umich.edu. Fax 734-647-4865.

### Notes

The authors declare no competing financial interest.

## ACKNOWLEDGMENTS

This research is supported by the Office of Naval Research (N00014-12-1-0452 and N00014-10-1-0348).

## REFERENCES

- (1) Banerjee, I.; Pangule, R. C.; Kane, R. S. *Adv. Mater.* **2011**, *23*, 690–718.
- (2) Ma, H.; Hyun, J.; Stiller, P.; Chilkoti, A. *Adv. Mater.* **2004**, *16*, 338–341.
- (3) Zhang, Z.; Chao, T.; Chen, S. F.; Jiang, S. Y. *Langmuir* **2006**, *22*, 10072–10077.
- (4) Ramsden, J. J. *Chem. Soc. Rev.* **1995**, *24*, 73–78.
- (5) Krishnan, S.; Weinman, C. J.; Ober, C. K. *J. Mater. Chem.* **2008**, *18*, 3405–3413.
- (6) Gudipati, C. S.; Finlay, J. A.; Callow, J. A.; Callow, M. E.; Wooley, K. L. *Langmuir* **2005**, *21*, 3044–3053.
- (7) Weinman, C. J.; Gunari, N.; Krishnan, S.; Dong, R.; Paik, M. Y.; Sohn, K. E.; Walker, G. C.; Kramer, E. J.; Fischer, D. A.; Ober, C. K. *Soft Matter* **2010**, *6*, 3237–3243.
- (8) Weinman, C. J.; Finlay, J. A.; Park, D.; Paik, M. Y.; Krishnan, S.; Sundaram, H. S.; Dimitriou, M.; Sohn, K. E.; Callow, M. E.; Callow, J. A.; Handlin, D. L.; Willis, C. L.; Kramer, E. J.; Ober, C. K. *Langmuir* **2009**, *25*, 12266–12274.
- (9) Krishnan, S.; Ayothi, R.; Hexemer, A.; Finlay, J. A.; Sohn, K. E.; Perry, R.; Ober, C. K.; Kramer, E. J.; Callow, M. E.; Callow, J. A.; Fischer, D. A. *Langmuir* **2006**, *22*, 5075–5086.
- (10) van Zoelen, W.; Zuckermann, R. N.; Segalman, R. A. *Macromolecules* **2012**, *45*, 7072–7082.
- (11) Colak, S.; Tew, G. N. *Biomacromolecules* **2012**, *13*, 1233–1239.
- (12) Colak, S.; Tew, G. N. *Langmuir* **2012**, *28*, 666–675.
- (13) Dimitriou, M. D.; Zhou, Z. L.; Yoo, H. S.; Killips, K. L.; Finlay, J. A.; Cone, G.; Sundaram, H. S.; Lynd, N. A.; Barteau, K. P.; Campos, L. M.; Fischer, D. A.; Callow, M. E.; Callow, J. A.; Ober, C. K.; Hawker, C. J.; Kramer, E. J. *Langmuir* **2011**, *27*, 13762–13772.
- (14) Sundaram, H. S.; Cho, Y.; Dimitriou, M. D.; Finlay, J. A.; Cone, G.; Williams, S.; Handlin, D.; Gatto, J.; Callow, M. E.; Callow, J. A.; Kramer, E. J.; Ober, C. K. *ACS Appl. Mater. Interfaces* **2011**, *3*, 3366–3374.
- (15) Shen, Y. R. *J. Phys. Chem. C* **2012**, *116*, 15505–15509.
- (16) Gracias, D. H.; Chen, Z.; Shen, Y. R.; Somorjai, G. A. *Acc. Chem. Res.* **1999**, *32*, 930–940.
- (17) Liu, Y. W.; Jasensky, J.; Chen, Z. *Langmuir* **2012**, *28*, 2113–2121.
- (18) Howell, C.; Diesner, M. O.; Grunze, M.; Koelsch, P. *Langmuir* **2008**, *24*, 13819–13821.
- (19) Zhang, C.; Myers, J. N.; Chen, Z. *Soft Matter* **2013**, *9*, 4738–4761.
- (20) Hankett, J. M.; Liu, Y. W.; Zhang, X. X.; Zhang, C.; Chen, Z. *J. Polym. Sci., Part B: Polym. Phys.* **2013**, *51*, 311–328.
- (21) Li, G. F.; Ye, S.; Morita, S.; Nishida, T.; Osawa, M. *J. Am. Chem. Soc.* **2004**, *126*, 12198–12199.
- (22) Ye, S. J.; Liu, G. M.; Li, H. C.; Chen, F. G.; Wang, X. W. *Langmuir* **2012**, *28*, 1374–1380.
- (23) Leung, B. O.; Yang, Z.; Wu, S. S. H.; Chou, K. C. *Langmuir* **2012**, *28*, 5724–5728.

- (24) Liu, Y. W.; Leng, C.; Chisholm, B.; Stafslie, S.; Majumdar, P.; Chen, Z. *Langmuir* **2013**, *29*, 2897–2905.
- (25) Ye, S. J.; Majumdar, P.; Chisholm, B.; Stafslie, S.; Chen, Z. *Langmuir* **2010**, *26*, 16455–16462.
- (26) Ye, S. J.; McClelland, A.; Majumdar, P.; Stafslie, S. J.; Daniels, J.; Chisholm, B.; Chen, Z. *Langmuir* **2008**, *24*, 9686–9694.
- (27) Leng, C.; Liu, Y. W.; Jenkins, C.; Meredith, H.; Wilker, J. J.; Chen, Z. *Langmuir* **2013**, *29*, 6659–6664.
- (28) Even, M. A.; Chen, C. Y.; Wang, J.; Chen, Z. *Macromolecules* **2006**, *39*, 9396–9401.
- (29) Wang, J.; Woodcock, S. E.; Buck, S. M.; Chen, C. Y.; Chen, Z. *J. Am. Chem. Soc.* **2001**, *123*, 9470–9471.
- (30) Lee, B. S.; Lee, J. K.; Kim, W. J.; Jung, Y. H.; Sim, S. J.; Lee, J.; Choi, I. S. *Biomacromolecules* **2007**, *8*, 744–749.
- (31) Li, L. Y.; Chen, S. F.; Zheng, J.; Ratner, B. D.; Jiang, S. Y. *J. Phys. Chem. B* **2005**, *109*, 2934–2941.
- (32) Zheng, J.; Li, L. Y.; Chen, S. F.; Jiang, S. Y. *Langmuir* **2004**, *20*, 8931–8938.
- (33) Ye, S. J.; Nguyen, K. T.; Boughton, A. P.; Mello, C. M.; Chen, Z. *Langmuir* **2009**, *26*, 6471–6477.
- (34) Keefe, A. J.; Brault, N. D.; Jiang, S. Y. *Biomacromolecules* **2012**, *13*, 1683–1687.
- (35) Zhang, Z.; Vaisocherova, H.; Cheng, G.; Yang, W.; Xue, H.; Jiang, S. Y. *Biomacromolecules* **2008**, *9*, 2686–2692.
- (36) Yang, W.; Xue, H.; Li, W.; Zhang, J. L.; Jiang, S. Y. *Langmuir* **2009**, *25*, 11911–11916.